Chemistry & Biology, Vol. 12, 1169–1178, November, 2005, ©2005 Elsevier Ltd All rights reserved. DOI 10.1016/j.chembiol.2005.08.006

A Photoactivable Probe for Calcium Binding Proteins

Adrian Israelson,[1] Laetitia Arzoine,[1] Salah Abu-hamad,[1] Vladimir Khodorkovsky,[2,3] and Varda Shoshan-Barmatz[1,*]
[1]Department of Life Sciences and The Zlotowski Center for Neuroscience
[2]Department of Chemistry
Ben-Gurion University of the Negev
Beer-Sheva 84713
Israel
[3]Université de la Méditerranée
UMR CNRS 6114
13288 Marseille 09
France

Summary

Ca^{2+} as a signaling molecule carries information pivotal to cell life and death via its reversible interaction with a specific site in a protein. Although numerous Ca^{2+}-dependent activities are known, the proteins responsible for some of these activities remain unidentified. We synthesized and characterized a photoreactive reagent, azido ruthenium (AzRu), which interacts specifically with Ca^{2+} binding proteins and strongly inhibits their Ca^{2+}-dependent activities, regardless of their catalytic mechanisms or functional state as purified proteins, embedded in the membrane or in intact cells. As expected from a Ca^{2+} binding protein-specific reagent, AzRu had no effect on Ca^{2+}-independent and Mg^{2+}-dependent activities. $Az^{103}Ru$ covalently bound, and specifically labeled, known Ca^{2+} binding proteins. AzRu is a photoreactive reagent that provides an approach for identification of Ca^{2+} binding proteins, characterization of their binding sites, and exploration of new Ca^{2+}-dependent processes.

Introduction

Ca^{2+} is a ubiquitous intracellular signal carrier responsible for controlling numerous cellular processes [1, 2]. Changes in cytosolic free calcium concentrations, $[Ca^{2+}]i$, have been associated with the regulation of a wide variety of cellular processes as important and disparate as cell differentiation, transport, motility, gene expression, metabolism, cell cycle activities, and pathogenesis [1].

At rest, $[Ca^{2+}]i$ is about 100 nM, but in response to different signals, this level can rise to ~1000 nM. Intracellular $[Ca^{2+}]$ is tightly controlled by an array of channels, pumps, and exchangers that represent ON and OFF systems [3]. The ON mechanisms feed Ca^{2+} into the cytoplasm from internal and external sources. Ca^{2+} is released from the endoplasmic reticulum (ER)/sarcoplasmic reticulum (SR) by the inositol-1,4,5-trisphosphate receptors and the ryanodine receptors (RyRs) [4], and from mitochondria by efflux systems [3]. Ca^{2+} enters the cell through voltage-dependent Ca^{2+} channels [5]. The OFF mechanisms turn calcium signaling off by rapid removal of Ca^{2+} from the cytoplasm by various pumps [6] and exchangers [7]. The plasma membrane Ca^{2+}-ATPase and Na^+/Ca^{2+} exchangers extrude Ca^{2+} to the outside, whereas the SR/ER Ca^{2+}-ATPase pumps Ca^{2+} to the internal stores.

Ca^{2+} performs its various tasks through binding to specific Ca^{2+} binding proteins, distinguished as Ca^{2+} buffers, Ca^{2+} sensors, and Ca^{2+}-activated proteins on the basis of their functions [1]. The Ca^{2+} sensors (i.e., troponin C, calmodulin) respond to an increase in $[Ca^{2+}]i$ by activating diverse processes, the Ca^{2+} buffers (i.e., calsequestrin, parvalbumin) control free $[Ca^{2+}]$, and Ca^{2+}-activated proteins (i.e., protein kinase C, Ca^{2+}-ATPases, calpain, NO synthase) are enzymatically active only in the presence of Ca^{2+}. Isocitrate-, α-ketoglutarate-, and pyruvate dehydrogenases are activated via different mechanisms in response to an increased mitochondrial $[Ca^{2+}]$ [8].

Fundamental to the understanding of normal and abnormal calcium signaling is the knowledge of the proteins involved. Several dozens of Ca^{2+} binding proteins have been identified, purified, and characterized, and their functions have been established. However, as judged by the significant amount of Ca^{2+}-dependent activities in which the participants are unknown, many Ca^{2+} binding proteins are yet unidentified. For example, mitochondria contain several different systems for transporting Ca^{2+}: the ruthenium red (RuR)-sensitive uniporter, Na^+-dependent and -independent efflux mechanisms, and the rapid mode of uptake [9]. None of the proteins responsible for these activities has been identified. Thus, an important step in elucidating calcium-signaling mechanisms involves identifying new Ca^{2+} binding proteins in order to discover their cellular localization and function in the cell.

Extensive studies have focused on developing specific Ca^{2+} binding reagents for probing changes in $[Ca^{2+}]i$ during cell function; fewer efforts, however, have been made to probe Ca^{2+} binding sites in proteins. In addition, despite advances in defining Ca^{2+} binding proteins, considerable experimental difficulties still remain in locating their Ca^{2+} binding sites [10].

In this study, we synthesized and characterized a novel, to our knowledge, photoreactive reagent—azido ruthenium (AzRu)—that interacts specifically with Ca^{2+} binding proteins and inhibits their activities. Radioactive $Az^{103}Ru$ covalently and specifically binds to Ca^{2+} binding proteins.

Results

With the aim of identifying new Ca^{2+} binding proteins and their Ca^{2+} binding sites, we synthesized a photoreactive reagent, AzRu, containing ruthenium and a photoactivable azido group, which can irreversibly interact with calcium binding proteins. We chose to synthesize this reagent since azido is a photoreactive group and

*Correspondence: vardasb@bgu.ac.il

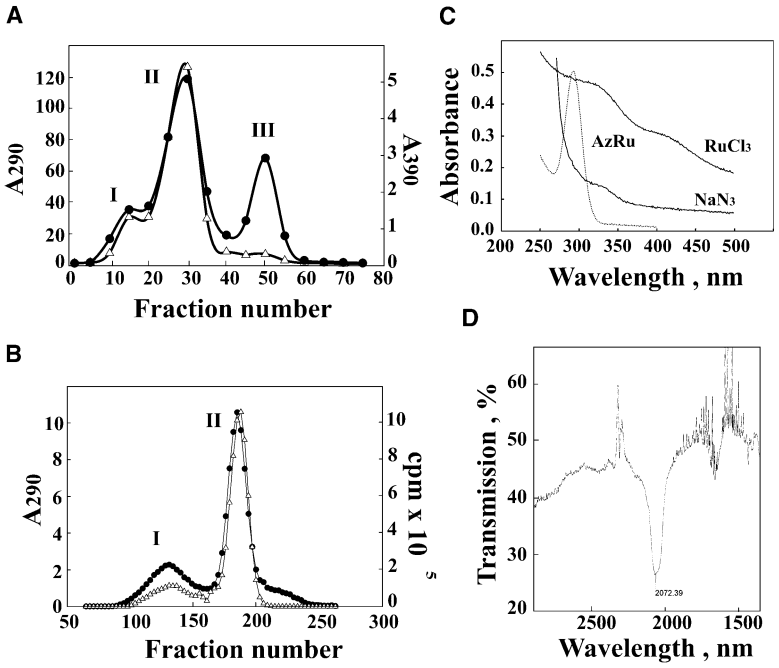

Figure 1. Purification and Characterization of AzRu

(A) AzRu was synthesized and purified by using a Sephadex LH-20 column. The absorbance at 290 nm (open triangles) represents AzRu (peak II) and at 390 nm (closed circles) represents that of another compound eluted from the column (peak III) with no effect on Ca^{2+}-dependent activities.

(B) $Az^{103}Ru$ was synthesized and purified in the same manner as AzRu, showing a similar elution profile as followed by radioactive counting (closed circles) or absorbance at 290 nm (open triangles).

(C) UV spectra of AzRu, $RuCl_3$, and NaN_3.

(D) IR spectrum of AzRu.

ruthenium-containing compounds such as RuR (see [11]) and Ru360 [12, 13] have been shown to interact with Ca^{2+} binding proteins and inhibit their activities.

Synthesis, Purification, and Characterization of AzRu

AzRu, purified by using a Sephadex LH –20 column (Figure 1A, peak II), has a maximal absorbance at 290 nm, distinct from that of the precursors NaN_3 or $RuCl_3$ (Figure 1C) and of RuR (data not shown). Compounds corresponding to peak I and peak III (λmax = 390 nm) had weak or no effect, respectively, on Ca^{2+}-dependent activities and, therefore, were not further characterized. The infrared spectrum of AzRu showed the characteristic band corresponding to the asymmetric azide stretching mode at ~2072 cm^{-1} (Figure 1D). Such a high wave number is characteristic of dinuclear μ-N_3 complexes rather than the terminal N_3 groups [14]. The elemental analyses (for O, Na, Cl, N, Ru) were performed for several samples. The samples exhibited identical IR and UV-Vis spectra and a constant percent ratio of Ru:N of 4.8:1. However, some amount of NaCl and water are also present, and their quantity varies depending on purification conditions and the quantity of moisture absorbed by the hygroscopic material. Based on the spectral features and the elemental analyses, we propose the formula of $Ru_2N_3Cl_5(H_2O)_n$, where n = 5–10. Interestingly, a similar ruthenium azide compound was prepared by Vrestal et al. in 1960 [15]. It was not isolated and was characterized by its absorption at 290 nm.

A radioactive $Az^{103}Ru$ was also synthesized and purified (Figure 1B), and its specific activity was used to estimate its concentration. Thus, its absorbance at 290 nm could be used to determine the molar absorbance coefficient of ~15,000 for AzRu. AzRu is soluble in water, and its activity was preserved for over 6 months.

AzRu Interacts Specifically with Ca^{2+} Binding Proteins

The specific interaction of AzRu with Ca^{2+}-dependent proteins was demonstrated by testing its effects on the activities of a variety of known Ca^{2+}-dependent and Ca^{2+}-independent proteins as summarized in Table 1. Inhibition by AzRu was observed for various Ca^{2+}-dependent proteins with different catalytic mechanisms.

Inhibition of the SR Calcium Pump, (Ca^{2+} + Mg^{2+})ATPase, by AzRu Is Highly Enhanced by UV Irradiation

The inhibition of Ca^{2+} accumulation by AzRu was dependent on AzRu concentration (Figures 2A and 2C) and on time of incubation with or without UV irradiation (Figure 2B). When SR membranes were exposed for 2 min to UV in the presence of AzRu, Ca^{2+} accumulation was inhibited with a half-maximal inhibition (IC_{50}) of about 1 μM, while, without UV, the IC_{50} was 4 μM AzRu (Figure 2A). However, increasing the UV exposure time to over 2 min enhanced the AzRu inhibition of the SR Ca^{2+} accumulation (Figure 2B). Moreover, UV irradiation for 20 min decreased the IC_{50} for AzRu inhibition of Ca^{2+} accumulation by about 140-fold to 7 nM (Figure 2C), suggesting photoactivation and irreversible binding of AzRu to the protein. The photochemical mechanism probably involves ejection of N_2 and unmasking of a highly reactive nitrene species, as described before [16]. UV irradiation of the SR membranes had no effect on the control activity or on the inhibition by AzRu added to the irradiated membranes in the dark (data not shown). In contrast to AzRu inhibition of SR Ca^{2+} accumulation, RuR and Ru360 had no inhibitory effect, but rather, stimulated accumulation (Figure 2A and Table 2). The difference between the effects of Ru360 and AzRu on the net Ca^{2+} accumulation is due to the different sensitivity of the Ca^{2+}-ATPase to the two reagents. Ru360 had no effect on Ca^{2+} accumulation by the SR (Figure 2A). On the other hand, Ru360 (2–4 μM) inhibited ryanodine binding to the SR Ca^{2+}

Table 1. AzRu Specifically Inhibits Ca^{2+}-Dependent Activities

Activity Assayed	Activity (% of Control) AzRu (20 μM)	AzRu (100 μM)	Divalent Cation Involved
1. Ca^{2+} uptake in SR (SERCA)	13 ± 6		Ca^{2+}
2. Ca^{2+} uptake in mitochondria	11 ± 4		
3. Ryanodine binding by SR RyR	18 ± 6		
4. VDAC conductance	19 ± 5		
5. Peroxidase	39 ± 4		
6. CaMKII-dependent GAPDH	6 ± 2		
7. Ca^{2+}-dependent mitochondrial swelling[a]	0		
8. Yeast hexokinase	77 ± 5	64 ± 4	Mg^{2+}
9. Brain hexokinase	73 ± 7	61 ± 3	
10. Pyruvate kinase	97 ± 7	81 ± 6	
11. Luciferase	97 ± 1	67 ± 3	
12. (Na^+/K^+)ATPase	92 ± 5	71 ± 4	
13. K^+ channel (KCNK0)	100 ± 0.3		Zn^{2+}
14. Glutamate dehydrogenase[b]		101 ± 5	None
15. Lactate dehydrogenase		91 ± 4	
16. G-6-P dehydrogenase		101 ± 7	
17. GA3P dehydrogenase		102 ± 5	
18. Alkaline phosphatase		86 ± 5	
19. Succinate-cytochrome c oxido-reductase		95 ± 5	
20. Lysozyme		101 ± 3	
21. Aldolase		78 ± 7	
22. Catalase		118 ± 8	
23. Choline oxidase		85 ± 3	

Summary of the effects of AzRu on different activities representing Ca^{2+}-, Mg^{2+}-, or Zn^{2+}-dependent or -independent proteins. Protein activity was assayed, in the dark, in the absence and the presence of different concentrations of AzRu as described in Experimental Procedures, and the degree of inhibition by 20 or 100 μM AzRu is presented. The results are the mean ± SEM of 3–6 experiments.
[a] PTP opening was completely inhibited at this concentration of AzRu (see Figure 3B).
[b] The enzyme possesses Ca^{2+} binding site(s) that are not involved in its activity.

release channel (Figure 2D); thus, Ca^{2+} release was inhibited and the net accumulation of Ca^{2+} was thereby increased. AzRu inhibited both activities at the same concentration range (Figure 2).

As proposed [17], the stimulatory effect of RuR on Ca^{2+} accumulation may result from inhibiting Ca^{2+} release mediated by the Ca^{2+} release channel/ryanodine receptor (RyR), and thus suggests that at the concentrations used, RuR and Ru360 had no effect on the (Ca^{2+}/Mg^{2+})ATPase activity.

Inhibition by AzRu of Ryanodine Binding to SR RyR

RyR, known as the intracellular Ca^{2+} release channel, possesses regulatory Ca^{2+} binding sites that are required for binding of the toxic alkaloid ryanodine, and this binding is inhibited by RuR [4]. AzRu strongly inhibited the Ca^{2+}-dependent specific binding of [^{3}H]ryanodine to its receptor in SR (Figure 2D). With no photoactivation, half-maximal inhibition was obtained at about 2 μM, and 80% inhibition was obtained at 20 μM AzRu (Figure 2D). At 2 μM, Ru360 had no effect on ryanodine binding, and at 20 μM, it inhibited binding partially (35%).

Inhibition of Ca^{2+} Accumulation in Mitochondria

The mitochondrial electron transfer from succinate to cytochrome c was not affected by AzRu, although it involves several electron transfer complexes containing dozens of polypeptides (Figure 3A). On the other hand, Ca^{2+} transport, which is carried out by a yet unidentified uniporter protein requiring that membrane potential be established by the electron transport chain, was strongly inhibited by AzRu, indicating the specificity of this reagent for Ca^{2+} binding proteins.

The opening of the permeability transition pore (PTP) in energized mitochondria, as induced by mitochondrial Ca^{2+} overload and monitored by mitochondrial swelling, was completely prevented by AzRu (Figure 3B). Inhibition of PTP opening by AzRu was also obtained when it was added after Ca^{2+} accumulation had reached a maximal level (Figure 3C); this suggests that AzRu interacts not only with the Ca^{2+} uniporter, but also with a component of the PTP, such as the voltage-dependent anion channel (VDAC) [18].

AzRu-Induced VDAC Channel Closure

VDAC is a channel protein that possesses Ca^{2+} binding sites and transports Ca^{2+} across the mitochondrial outer membrane [11]. Channel activity of purified VDAC reconstituted into a planar lipid bilayer was measured by the ions passing current across the bilayer in response to a voltage gradient of −10 mV, as a function of time (Figure 3E). In the absence of AzRu, VDAC is stable in a long-lived, fully opened state and remains open for up to 2 hr of recording. However, addition of AzRu to the same channel induced VDAC closure in a time-dependent manner (Figure 3E). Ca^{2+}, in the presence of 1 M NaCl, prevented the inhibitory effect of AzRu on VDAC activity. As has been shown for RuR [11], chelation of Ca^{2+} with EGTA reestablished AzRu inhibition, suggesting specific interaction of AzRu with VDAC Ca^{2+} binding sites. AzRu also decreased VDAC conductance in multichannel experiments at all voltages tested and stabilized VDAC conductance at a constant low level regardless of the voltage gradient applied (Figure 3D). Similar results have been obtained with RuR and Ru360 [18].

Inhibition by AzRu of CaM Kinase IIβ_M-Dependent GAPDH Activity

The muscle-specific CaM kinase IIβ_M stimulates the activity of GAPDH by 3- to 4-fold in a Ca^{2+}/calmodulin-dependent manner [19]. AzRu inhibited the activity of CaM kinase IIβ_M-dependent GAPDH activity, with 50% inhibition occurring at 5 μM AzRu and complete inhibition occurring at 20 μM AzRu. AzRu had no effect on the activity of the enzyme in a Ca^{2+}/calmodulin-free medium (Table 1), suggesting that inhibition occurs via interaction with calmodulin. Horseradish peroxidase, a Ca^{2+} binding protein [20], was also inhibited by AzRu (Table 1).

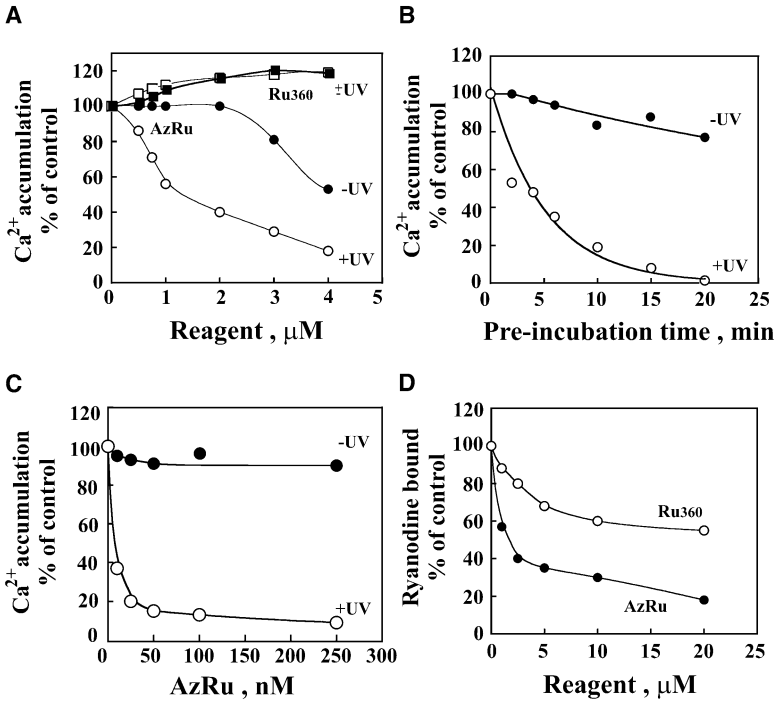

Figure 2. AzRu Inhibits the Ca^{2+} Pump and Ryanodine Binding in Isolated SR: Evidence for Photoactivation

(A) SR was incubated for 10 min at 24ºC with the indicated concentration of Ru360 (open squares) or AzRu (open circles), with (open circles and squares) or without (closed circles and squares) 2 min of UV irradiation.

(B) SR was incubated with 1 μM AzRu for the indicated time, with (open circles) or without (closed circles) UV irradiation.

(C) SR was incubated for 20 min with the indicated concentration of AzRu with (open circles) or without (closed circles) UV irradiation. Samples from (A), (B), and (C) were assayed for Ca^{2+} accumulation. Control activities (100%) were: 2.4, 2.5, and 2.1 μmol/mg protein/min for (A), (B), and (C), respectively. The samples that were not exposed to UV were kept in the dark during all experiments, and those exposed to UV were stirred during the incubation time.

(D) [^{3}H]Ryanodine binding to SR was assayed following 10 min of incubation in the dark of SR (1 mg/ml) with the indicated concentration of AzRu (closed circles) or Ru360 (open circles). Control activity (100%) = 3.0 pmol ryanodine bound/mg of protein. The results are a representative experiment of 3–4 similar experiments with different reagent and SR preparations.

Ca^{2+}-Independent Reactions Are Not Affected by AzRu

The results, summarized in Table 1, indicate that the activities of 16 different Ca^{2+}-independent proteins, such as glucose-6-phosphate dehydrogenase, lactate dehydrogenase, alkaline phosphatase, GAPDH, aldolase, catalase, lysozyme, choline oxidase, and over two dozen polypeptides involved in electron transfer in mitochondria, were not or were only slightly inhibited by AzRu (<10% at 100 μM). In contrast, the activities of calcium-dependent proteins were strongly inhibited by AzRu (>90% at $\leq$ 20 μM). The results also indicate that the activities of Mg^{2+}-dependent proteins, such as yeast and brain hexokinase, pyruvate kinase, luciferase, and (Na^+/K^+)ATPase, as well as that of the Zn^{2+}-sensitive KCNK0 channel, were not affected or were weakly inhibited at high AzRu concentrations (~30% at 100 μM). These results strongly support the specific interaction of AzRu with Ca^{2+} binding proteins.

$Az^{103}Ru$ Specifically Labeled Ca^{2+} Binding Proteins

Next, we synthesized radiolabeled $Az^{103}Ru$ and employed it as a photoaffinity label for Ca^{2+} binding proteins in SR and mitochondria (Figure 4). UV irradiation of SR or mitochondria in the presence of $Az^{103}Ru$ resulted in its covalent binding to several proteins, as revealed by SDS-PAGE followed by Coomassie staining and autoradiography. As expected for the photoreactive $Az^{103}Ru$, the labeling of the proteins was significantly increased upon UV irradiation, indicating the formation of a stable covalent bond. In skeletal muscle SR incubated with 0.5–2 nmol $Az^{103}Ru$/mg protein (0.5–2 μM) with UV irradiation, 10 out of about 30 proteins stained by Coomassie were labeled with $Az^{103}Ru$. Among the labeled proteins are known Ca^{2+} binding proteins such as RyR, myosin, Ca^{2+}-ATPase, and calsequestrin, but there were also two unidentified proteins of 29 and 25 kDa (Figure 4A). Similarly, in an isolated mitochondrial membranal fraction from which

Table 2. Comparison of RuR, Ru360, and AzRu Sensitivity of Different Ca^{2+}-Dependent Activities

	IC_{50}, μM		
Assay	RuR	Ru360	AzRu[a]
Ca^{2+} accumulation in SR	No inhibition[b]	No inhibition[b]	4.91 ± 0.055
Ca^{2+} accumulation in mitochondria	0.16 ± 0.03	0.067 ± 0.008	1.78 ± 0.12
Ryanodine binding in SR	7.2 ± 0.55	14.8 ± 2.8	2.9 ± 0.17

Ca^{2+} accumulation in SR and mitochondria was assayed as described in Experimental Procedures in the absence and presence of different concentrations of RuR (0.05–100 μM), Ru360 (0.01–100 μM), or AzRu (0.1–100 μM). The concentration required for 50% inhibition (IC_{50}) was derived from the plot of Ca^{2+} accumulation activity or ryanodine binding as a function of the reagent concentration. The results are the mean ± SEM of 3–5 experiments.

[a] Inhibition by photoactivated AzRu is not present in (see Figures 2A and 2C).

[b] No inhibition; rather, stimulation was obtained.

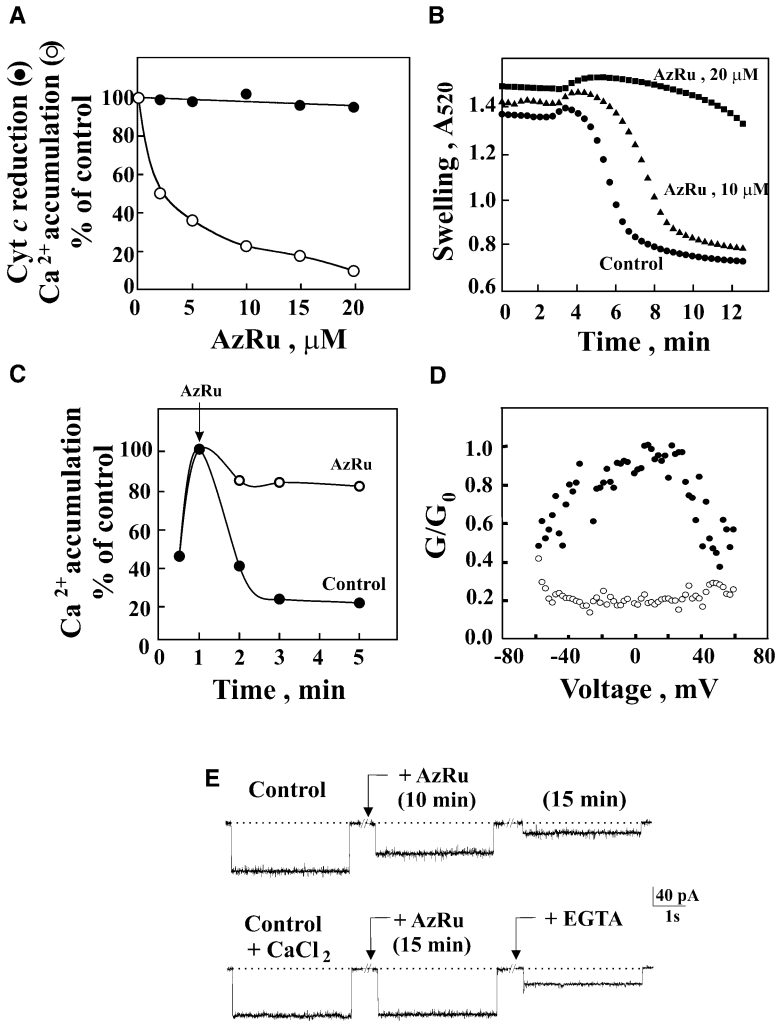

Figure 3. Ca^{2+} Uptake, but Not Electron Transport, Is Inhibited by AzRu in Isolated Mitochondria

(A) Electron transport (ET) from succinate to cytochrome c (closed circles) and Ca^{2+} accumulation (open circles) were assayed after 10 min of incubation of the mitochondria in the dark at 24°C with the indicated concentration of AzRu. Control activities (100%) were 134 nmol/mg protein and 130 nmol/mg protein for Ca^{2+} accumulation and ET, respectively.

(B) Ca^{2+}-induced mitochondrial swelling was assayed in the absence or in the presence of 10 or 20 μM AzRu. Swelling was initiated by the addition of Ca^{2+} (200 μM) to the sample and was monitored by following the change in absorbance at 520 nm.

(C) Mitochondria were exposed to Ca^{2+} accumulation conditions, and their Ca^{2+} content was assayed at the indicated times. AzRu (20 μM) was added 1 min after Ca^{2+} accumulation was initiated and had reached a maximal level (indicated by the arrow).

(D) Multichannel recordings of the average steady-state conductance of VDAC before (closed circles) and 15 min after (open circles) the addition of 20 μM AzRu as a function of voltage are shown. Relative conductance was determined as the ratio of conductance at a given voltage (G) and the maximal conductance (Go). The experiments are representative of 4–5 similar experiments.

(E) AzRu inhibits VDAC channel activity in the absence, but not in the presence, of Ca^{2+}. VDAC was reconstituted into a PLB, and channel currents through VDAC, in response to a voltage step from 0 to −10 mV, were recorded before and 10 or 15 min after the addition of AzRu (20 μM). Where indicated, VDAC was exposed to 20 μM AzRu in the presence of 5 mM $CaCl_2$, and recordings were made at the indicated time or 2 min after the addition of the indicated compounds. Recordings were also made 5 min after the addition of EGTA to a final concentration of 6 mM. The dashed lines indicate zero current.

soluble proteins were extracted, photoactivated $Az^{103}Ru$ labeled 7 out of about 27 proteins stained by Coomassie (Figure 4B). Weak $Az^{103}Ru$ labeling of the proteins was observed with no UV irradiation, indicating a very stable interaction. This finding is not surprising when considering the reported labeling of mitochondrial proteins with the nonphotoreactive reagent $^{103}Ru360$ [13]. Photoactivated $Az^{103}Ru$ labeled in a concentration-dependent manner purified calsequestrin and calmodulin, known Ca^{2+} binding proteins (Figure 4C). Moreover, purified VDAC was labeled with $Az^{103}Ru$, and this labeling was strongly reduced by preincubation of VDAC with 1 mM $CaCl_2$ or 100 μM Ru360, indicating the specificity of AzRu for VDAC Ca^{2+} binding sites (Figure 4D).

AzRu Protects against Apoptosis Induced by Staurosporine or by Overexpression of Native VDAC, but Not E72Q-Mutated VDAC

RuR has been shown to protect against apoptotic cell death induced by various stimuli in different cell types (see [21]). Recently, we demonstrated that this RuR protection against cell death is a result of RuR interaction with VDAC, since it was not observed in E72Q-mutated VDAC [21]. Exposure of U-937 cells to staurosporine (STS) for 5 or 7 hr resulted in apoptotic cell death of about 42% and 76% of the cells, respectively, whereas only 6% of the STS nonexposed cells died. AzRu, added 18 hr before exposure to STS, dramatically reduced STS-activated apoptotic cell death by about 75% and 47% in cells exposed to STS for 5 and 7 hr, respectively. AzRu had no effect on the viability of the cells that were not exposed to STS (Figures 5A and 5B).

To further investigate the relationship between the protective effect of AzRu and its interaction with VDAC, U-937 cells were transfected with native mVDAC or E72Q-mutated mVDAC1, and the effect of AzRu on apoptotic cell death was examined. As shown previously [21], transfecting cells with native or E72Q-mutated mVDAC1 resulted in apoptotic cell death (75%-80%), as characterized by enhanced nuclear fragmentation. In contrast, untransfected cells showed 5%–8% cell

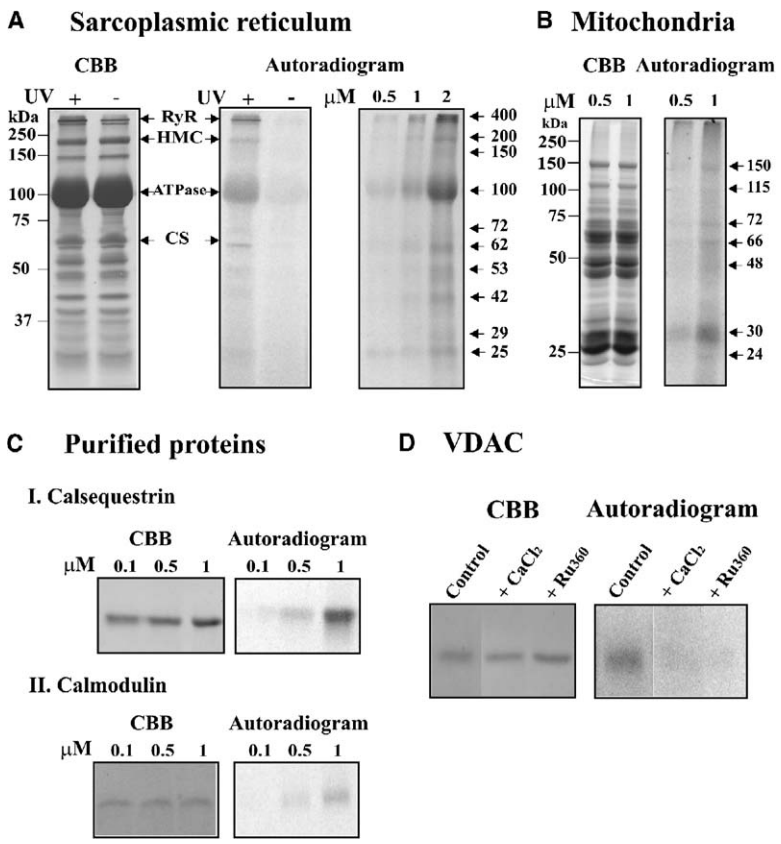

Figure 4. $Az^{103}Ru$ Labels SR and Mitochondrial Proteins

(A–C) (A) SR, (B) Na_2CO_3-extracted mitochondrial membranes, or (C) purified calmodulin or calsequestrin were incubated for 4 min in the dark (−UV) or were irradiated with UV in the presence of 0.5 μM or the indicated concentration of $Az^{103}Ru$ and subjected to SDS-PAGE, Coomassie staining (CBB), and autoradiography. RyR, RyR monomer; CS, calsequestrin; HMC, heavy myosin chain; ATPase, Ca^{2+}-ATPase. The molecular weight standards are presented, and the $Az^{103}Ru$-labeled proteins are indicated by arrowheads.

(D) Purified VDAC was irradiated for 4 min with UV in the presence of 0.5 μM $Az^{103}Ru$. Where indicated, VDAC was preincubated with 1 mM $CaCl_2$ or 100 μM Ru360 before the labeling with $Az^{103}Ru$.

death (Figure 5C). Preincubation of cells transfected with native mVDAC1 with 10 μM AzRu for 18 hr dramatically reduced their apoptotic cell death (71%–84% protection), while, in cells transfected with E72Q-mutated mVDAC, AzRu reduced apoptotic cell death by only 31%–34%. AzRu had no effect, nor did it even slightly increase apoptotic death in control cells. Thus, the results suggest that AzRu protection against apoptosis may be exerted through its direct interaction with VDAC.

Discussion

AzRu was synthesized in order to develop a photoreactive probe specific for Ca^{2+} binding proteins that could irreversibly interact with these proteins. Indeed, the results presented here show that the reagent fulfills the expected properties and suggest that AzRu can be of major interest in a wide range of biological studies. This includes identification of Ca^{2+} binding sites, and of new Ca^{2+} binding proteins and their functions, and discovering the involvement of Ca^{2+} in various biological phenomena. AzRu exerted its inhibitory effect on Ca^{2+}-dependent activities regardless of their catalytic mechanisms or of the functional state of the protein—purified, embedded in SR or mitochondrial membrane, or in intact cells.

Specificity of AzRu for Ca^{2+} Binding Proteins

The specific interaction of AzRu with Ca^{2+} binding proteins is reflected in the inhibition of their activities. Some of these proteins catalyze the transport of Ca^{2+} across the membrane by distinct mechanisms, all of which involve Ca^{2+} binding to the protein. Some examples are the Ca^{2+} pump that transports Ca^{2+} at the expense of ATP hydrolysis (Figures 2A–2C), the uniporter at the mitochondrial inner membrane that transports Ca^{2+} to the matrix and is driven by the membrane potential (Figure 3A), and the outer mitochondrial channel VDAC, which transports and binds Ca^{2+} [11] (Figures 3D and 3E). The reagent also interacted with regulatory Ca^{2+} binding sites, such as those of calmodulin and RyR (Table 1 and Figure 2D).

AzRu had no effect on Ca^{2+}-independent reactions and only slightly affected Mg^{2+}-dependent activities (Table 1), indicating the specificity of AzRu for Ca^{2+} binding proteins. The interaction of AzRu with Ca^{2+} binding sites is further supported by the results showing that the inhibition of VDAC channel activity by AzRu was prevented in the presence of Ca^{2+} and was reestablished upon Ca^{2+} removal (Figure 3E).

The results obtained with the radioactive $Az^{103}Ru$ further support its specificity for Ca^{2+} binding proteins. Upon photoactivation, $Az^{103}Ru$ covalently bound to several SR known Ca^{2+}-dependent proteins such as Ca^{2+}-ATPase, calsequestrin, and RyR. Mitochondria contain several Ca^{2+}-activated enzymes in the matrix [8] and possess Ca^{2+} influx and efflux activities catalyzed by as yet unidentified proteins [9]. In mitochondrial membranes free of soluble proteins, about seven proteins were labeled with $Az^{103}Ru$, among them VDAC [11] and aralar [22], both possessing Ca^{2+} binding sites. AzRu binding to VDAC was inhibited in the presence of Ca^{2+}, indicating the specificity of AzRu for VDAC Ca^{2+} binding sites. These results indicate that,

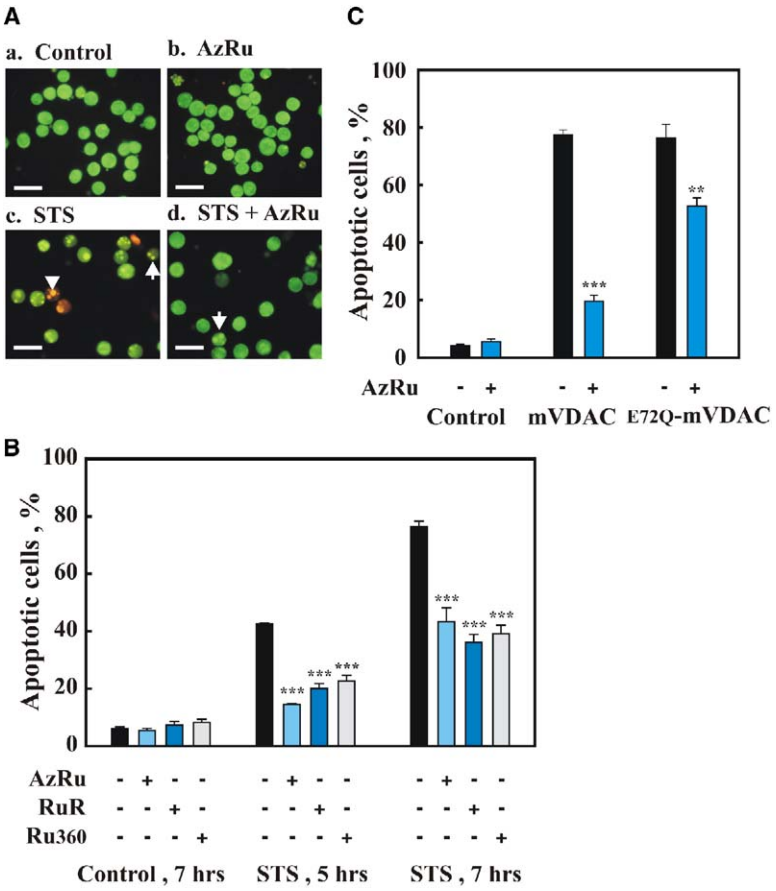

Figure 5. AzRu Protects against Apoptotic Cell Death Induced by STS or by Overexpression of Native, but Not E72Q-Mutated, VDAC

(A) U-937 cells were incubated (a and c) without or (b and d) with AzRu (10 μM) for 18 hr and thereafter were exposed to (c and d) STS (1.25 μM). After 5 hr, the cells were stained with acridine orange and ethidium bromide. Arrows indicate cells in an early apoptotic state, represented by a degraded nucleus (stained by acridine orange). Arrowheads indicate a late apoptotic state, as shown by the presence of a degraded nucleus (stained by both acridine orange and ethidium bromide). Scale bar, 20 μm.

(B) Quantitative analysis of apoptotic cell death in control cells and cells exposed to AzRu, RuR, and Ru360 (10 μM) was assessed 5 and 7 hr after their exposure to STS (1.25 μM) by ANOVA and a Student's t test. $p < 0.001$ was considered statistically significant (marked by three asterisks). Data are the means ± SEM of three independent experiments. In each independent experiment, approximately 200 cells were counted for each treatment.

(C) Quantitative analysis of cell death induced by native or E72Q-mutated VDAC1 overexpression. U-937 cells were transfected with a plasmid encoding native or E72Q-mutated VDAC1. AzRu (10 μM) was added to the cells 56 hr after transfection, and, 20 hr later, cell viability was analyzed by acridine orange/ethidium bromide staining as described in Experimental Procedures. ANOVA and a Student's t test were used, and $p < 0.001$ (marked by three asterisks) and $p < 0.01$ (marked by two asterisks) were considered statistically significant. Values represent the means ± SEM of three independent experiments.

indeed, the reagent is photoreactive and specifically binds to Ca^{2+} binding proteins. Thus, $Az^{103}Ru$ could be a useful tool for the identification of unidentified Ca^{2+} binding proteins, and for probing the location and possible structure of the Ca^{2+} binding sites.

Comparison of AzRu, RuR, and Ru360 Effects

The polycationic RuR and Ru360 have been employed in various studies as inhibitors of Ca^{2+}-dependent reactions (see [11]). In contrast to RuR and Ru360, AzRu is a photoreactive reagent, as reflected in its UV-enhanced inhibition, and increased apparent binding affinity by about 140-fold (Figure 2C). As shown here, even with no photoactivation, AzRu, in contrast to RuR and Ru360, was effective in inhibiting the SR Ca^{2+} pump (Figure 2A and Table 2). AzRu was also more effective than RuR or Ru360, with or without photoactivation, in inhibiting the Ca^{2+}-dependent binding of ryanodine to RyR (Figure 2D and Table 2). This may open the way to inhibit other Ca^{2+}-dependent activities that are not sensitive to RuR, such as the plasma membrane Ca^{2+}-ATPase.

The binding mechanism of AzRu to Ca^{2+} binding proteins is not yet defined. However, we assume that the same proposed mechanism for RuR and Ru360 applies to AzRu. Recently [23], using site-directed mutagenesis, it has been shown that RuR interconnects glutamate residues located in two subunits of the TASK-3 potassium channel and that this interaction is required for its inhibitory action. Thus, the reagent activity is dependent on the reagent charge and on the location of the charged Ru moiety in the molecule. This may explain why the cation Ru^{3+} is not an inhibitor, and may explain the differential effects of RuR, Ru360, and AzRu in inhibiting various Ca^{2+}-dependent activities (see Table 2). Thus, the mechanism by which ruthenium-containing compounds interact with Ca^{2+} binding proteins may involve interaction with several negatively charged residues located in a specific geometry.

In intact cells, RuR was shown to slowly cross the plasma membrane and to protect against cell death induced by various stimuli (see [21]). Similar to RuR and Ru360, AzRu protected against apoptotic cell death induced by STS (Figures 5A and 5B). Moreover, AzRu protected against apoptotic cell death induced by overexpression of native mVDAC1, but not E72Q-mutated mVDAC1 (Figure 5C), suggesting that AzRu is able to enter into the cell and that its protective effect is a result of its interaction with VDAC.

RuR was employed to improve mitochondrial production in ischemic reperfused pig myocardium [24], was employed in the nervous system to follow neuronal

death progress [25], and can act as an antioxidant under certain conditions [26]. Considering the potent activity of AzRu in RuR-insensitive reactions (see Table 2), its applications in various biological studies should be explored.

AzRu as a Powerful Tool to Assess Ca^{2+}-Dependent Cellular Processes

An important step toward elucidating Ca^{2+} signaling mechanisms and discovering the cellular localization and functions of the proteins involved is the identification of as many Ca^{2+} binding proteins as possible. To our knowledge, the photoreactive AzRu, developed in this study, is a novel affinity labeling reagent that has a high degree of specificity toward Ca^{2+} binding proteins and most probably interacts at or around the Ca^{2+} binding site of target proteins. Radioactive AzRu with its covalent binding capacity (Figure 4) can be used to identify Ca^{2+} binding proteins, such as the unidentified mitochondrial uniporter, and the proteins mediating Na^+-dependent and -independent efflux [9].

To conclude, the results of this study suggest that AzRu and Ca^{2+} share their protein binding sites and that AzRu, as a photoreactive reagent, could be used as a probe to determine the binding site of Ca^{2+}. This new, to our knowledge, reagent can be exploited in developing a novel methodological approach for the identification of new Ca^{2+} binding proteins and their Ca^{2+} binding sites, and in uncovering their functions.

Significance

To our knowledge, the present work reports the synthesis, characterization, and applications of the first photoreactive Ca^{2+} analog reagent, AzRu, that binds covalently to Ca^{2+} binding sites in proteins. The ubiquitous and pivotal role of Ca^{2+} in diverse physiological processes is evident. Ca^{2+} acts as a messenger, stimulating numerous processes vital to cell life and death. However, despite advances in defining Ca^{2+}-dependent activities, difficulties in detecting Ca^{2+} binding proteins still remain. The specificity of AzRu for Ca^{2+} binding proteins, its photoactivation, and its radioactive labeling pave the way for the wide use of AzRu as a powerful tool to assess Ca^{2+}-dependent cellular processes, both in vitro and in vivo. The reagent has a number of intriguing fundamental properties that may open new avenues to address various Ca^{2+}-dependent biological phenomena, among them protein-protein interactions. Indeed, novel AzRu-based optical biosensor chips are currently under development and will be used to search for new Ca^{2+} binding proteins and for the identification of specific protein complexes, by using a chip containing Ca^{2+} binding proteins. These would allow for the generation of a comprehensive Ca^{2+}-targeted protein database and detection of defective Ca^{2+} binding proteins involved in various diseases and disorders, potentially leading to identification of novel biomarkers for disease diagnostics. Furthermore, developing fluorescent AzRu derivatives as probes for the application of Ca^{2+} binding protein imaging in living cells (in progress) would allow us to follow Ca^{2+} binding protein distribution under specific conditions.

Experimental Procedures

Materials

Aldolase, alkaline phosphatase, ATP, bovine liver catalase, choline oxidase, CM-cellulose, n-decane, glucose 6-phosphate dehydrogenase, glutamate dehydrogenase, glyceraldehyde 3-phosphate dehydrogenase, HEPES, yeast hexokinase, lactate dehydrogenase, leupeptin, luciferase, mannitol, horseradish peroxidase, PMSF, pyruvate kinase, soybean asolectin, sucrose, Tris, and Triton X-100 were purchased from Sigma (St. Louis, MO, USA). [^{45}Ca], [^{103}Ru], and [^{3}H]ryanodine were purchased from NEN Life Science Products, Inc. (Boston, USA). Unlabeled ryanodine was obtained from Calbiochem. Sephadex LH-20 was purchased from Amersham Biosciences. n-Octyl-β-D-glucopyranoside (β-OG) was obtained from Bachem AG (Germany). Lauryl-(dimethyl)-amineoxide (LDAO) and ruthenium red (98% pure) were obtained from Fluka (Chemie, GmbH). Ruthenium chloride was purchased from Aldrich. Hydroxyapatite (Bio-Gel HTP) was purchased from Bio-Rad Laboratories (Hercules, CA), and Celite was purchased from Merck. Synthetic firefly D-luciferin reagent was purchased from Biosynth AG. Ru360 was synthesized according to Ying et al. [12].

UV-Vis spectra were recorded by an Ultraspec 2100 spectrophotometer, and IR spectra were recorded by a Nicolet 5ZDX instrument.

Synthesis, Purification, and Characterization of AzRu

$RuCl_3 \cdot 3H_2O$ (150 mg) was dissolved in 1.44 ml 6 N HCl, and 0.2 ml absolute ethanol was added. The solution was placed in a water bath at 95ºC in order to reduce any Ru (IV) normally present in commercial $RuCl_3 \cdot 3H_2O$. After 1 hr, NaN_3 (93.6 mg) and water were added, giving a final volume of 10 ml, and the solution was incubated for 4 hr at 95ºC in a sealed tube. The reaction solution was then loaded into a Sephadex LH-20 column (3 × 70 cm) previously equilibrated with water. The column was washed with water, and the fractions (3 ml) with maximal absorption at 290 nm (peak II) were combined and lyophilized to dryness. The product was then analyzed by TLC by using cellulose F plates and 0.16 M ammonium formate (pH 8.5) and 20% methanol as a developer. The peak II product migrated as a single spot with R_f = 0.9, distinct from the mobility of $RuCl_3$ (R_f = 0) and NaN_3 (R_f = 0.77). The purified product, azidoruthenium, has a maximal absorbance at 290 nm and a molar coefficient of ~15,000. The elemental analyses of different samples invariably showed a 4.8:1 molar ratio of Ru:N, corresponding to that of Ru_2N_3. However, some amount of NaCl was always present in the samples, and the content of Cl and water varied corresponding to the empirical formulas from $Ru_2N_3Cl_5 \times (nH_2O, mNaCl)$ where n = 5–10, m = 2–3 (the analyses for Ru, N, Cl, Na, and O were carried out by SGS Cervac Wolff, Service Analyses Elementaires, Evry, France).

Attempts to obtain AzRu crystals from a solution of methanol, ethanol, acetonitrile, diethyl ether, or their different combinations resulted in a hygroscopic powder or microcrystals that was not suitable for X-ray structure determination.

The radiolabeled AzRu was synthesized as described above for the nonradioactive reagent, by using 4.5 mg $RuCl_3$ (23.5 μmol) and 1 mCi ^{103}Ru. All additions were proportionately reduced at a final volume of 1.2 ml. The Sephadex LH-20 column dimensions were 1.5 × 40 cm. The yield of the synthesis was 5.4 μmol AzRu (about 44% of the Ru^{3+} used), with a specific activity of 200 cpm/pmol AzRu.

Membrane and Protein Preparations

SR membranes were prepared from rabbit fast twitch skeletal muscle as described by Saito et al. [27]. Mitochondria were isolated from rat liver as described previously [11]. Na_2CO_3-extracted mitochondrial membranes were obtained by incubation of rat liver mitochondria (5 mg/ml) with 50 mM Na_2CO_3 (pH 11) for 30 min at 4ºC, and the pellet obtained by centrifugation at 20,000 × g for 20 min was washed twice with 10 mM Tricine (pH 7.4). Protein concentration was determined according to Lowry [28].

Ca^{2+} Accumulation by SR or Mitochondrial Membranes

Mitochondrial $^{45}Ca^{2+}$ uptake by freshly isolated mitochondria (0.5 mg/ml) was assayed for 0.5–7 min at 30ºC in the presence of 225 mM mannitol, 75 mM sucrose, 120 μM $CaCl_2$ (containing 3 ×

10^4 cpm/nmol $^{45}Ca^{2+}$), 5 mM HEPES/KOH, 5 mM succinate, and 0.l mM Pi (pH 7.0) [11]. SR membranes (0.04 mg/ml) were incubated for 2–20 min with AzRu (10 nM to 5 μM) in the dark or were irradiated with a 15 W ultraviolet lamp in 20 mM Mops, 0.1 M KCl (pH, 6.8). $^{45}Ca^{2+}$ uptake by the SR was assayed for 2 min in the presence of 20 mM Mops, 0.1 M KCl, 1.5 mM $MgCl_2$, 1.5 mM ATP, 0.5 mM EGTA, 0.5 mM $CaCl_2$ (containing 3×10^4 cpm/nmol $^{45}Ca^{2+}$), and 50 mM Pi (pH 6.8) as described previously [29]. $^{45}Ca^{2+}$ uptake was terminated by rapid Millipore filtration followed by a wash with 5 ml of 150 mM KCl.

Mitochondrial Swelling

Ca^{2+}-induced mitochondrial swelling was assayed in freshly isolated mitochondria under the same conditions as those employed for Ca^{2+} accumulation, except that the reaction was performed at 24ºC. Swelling was initiated by the addition of Ca^{2+} (0.2 mM) to the sample cuvette. Absorbance changes at 520 nm were monitored every 15–20 s with an Ultraspec 2100 spectrophotometer.

[^{3}H]Ryanodine Binding

Ryanodine binding by SR membranes was assayed as described previously [10]. Membranes were incubated for 60 min at 37ºC in a standard binding solution containing 1 M NaCl, 20 mM Mops (pH 7.4), 50 μM free [Ca^{2+}], and 20 nM [^{3}H]ryanodine, followed by vacuum filtration of the sample through nitrocellulose filters (0.3 μm). Specific binding of [^{3}H]ryanodine was defined as the difference between the binding in the absence and the presence of 100 μM unlabeled ryanodine.

Protein Purifications

The voltage-dependent anion channel (VDAC) was extracted from mitochondria with 2% LDAO and was purified by using LDAO and a hydroxyapatite/Celite column followed by a carboxymethyl (CM)-cellulose column in which LDAO was replaced by 0.3% β-OG [18]. Rat brain hexokinase-I (HK-I) [30], sheep brain calmodulin [31], and egg lysozyme [32] were purified as described.

VDAC Channel Recording and Analysis

Reconstitution of the purified VDAC into a planar lipid bilayer (PLB), multichannel current recording, and data analyses were carried out as previously described [11]. Purified VDAC was added to the chamber defined as the *cis* side. Currents were recorded under voltage-clamp mode by using a Bilayer Clamp BC-525B amplifier and were measured with respect to the *trans* side of the membrane (ground).

Photoaffinity Labeling with $Az^{103}Ru$

SR, mitochondria, or purified proteins were irradiated with a 15 W ultraviolet lamp for 3–4 min in the presence of 100 nM-1 μM $Az^{103}Ru$ (200 cpm/pmol) in 40 μl of 20 mM Tricine (pH 7.4). The irradiated samples were subjected to SDS-PAGE [33], followed by Coomassie staining, and the dried gel was exposed directly to Kodak X-Omat film (Eastman Kodak Co.).

Potassium Channel Activity

Xenopus laveis oocytes were isolated and injected with 23 nl containing 0.2 ng cRNA KCNK0 as described [34]. Whole-cell currents were measured 2 days after injection by a two electrode voltage clamp (Axon Instruments, Union City, CA, USA). Data were filtered at 0.5 kHz and sampled at 2 kHz. The bath solution contained (in mM): 4 KCl, 96 NaCl, 1 $MgCl_2$, 0.3 $CaCl_2$, 5 HEPES/NaOH (pH 7.5). Oocytes were held at −80 mV, and currents were monitored every 5 s for 100 ms at +20 mV.

Tissue Culture and Induction of Apoptotic Cell Death

The U-937 human monocytic cell line was grown under an atmosphere of 95% air and 5% CO_2 in RPMI 1640 supplemented with 10% fetal calf serum (FCS), 1 mM L-glutamine, 100 U/ml penicillin, and 100 μg/ml streptomycin. Cells were plated at a density of 5.4×10^4 cells/cm^2 in 24-well plates and were then incubated with or without AzRu for 18 hr before exposure to 1.25 μM staurosporine (STS) to induce apoptosis. Cell viability was analyzed 5 and 7 hr after STS addition by staining with 100 μg/ml acridine orange (AcOr) and 100 μg/ml ethidium bromide (EtBr) in PBS [21]. The cells were then visualized by fluorescence microscopy (Olympus IX51), and images were recorded on an Olympus DP70 camera, with an SWB filter. For cell transfection, logarithmically growing U-937 cells were resuspended in RPMI 1640 supplemented with 10% FCS, 100 U/ml penicillin, and 100 μg/ml streptomycin at a concentration of 2.5×10^7 cells/ml and were transfected with pEGFP-mVDAC1 or pEGFP-E72Q-mVDAC1. Transfection was performed by electroporation with a single pulse from a Bio-Rad micropulser II with a capacitance extender unit (200 V, 950 μF). Cells were incubated on ice for 10 min before and after transfection, and then resuspended in 20 ml RPMI 1640 supplemented with 10% FCS, 1 mM l-glutamine, 100 U/ml penicillin, and 100 μg/ml streptomycin. Transfection efficiencies were 68%–72%, as assessed by GFP expression. GFP-positive cells were viewed under a fluorescence microscope (Olympus IX51) with a blue filter.

Enzymatic Activities

Glyceraldehyde 3-phosphate dehydrogenase (GAPDH), aldolase, lactate dehydrogenase, pyruvate kinase [19], rat brain hexokinase-I, yeast hexokinase [30], glucose 6-phosphate dehydrogenase, and glutamate dehydrogenase activities were carried out at room temperature by monitoring spectrophotometrically the reduction of NAD^+ or the oxidation of NADH at 340 nm by using an Ultraspec 2100 spectrophotometer.

Alkaline phosphatase activity was assayed by using p-nitrophenyl phosphate as a substrate, and the formation of p-nitrophenol was monitored spectrophotometrically at 410 nm as previously described [35].

Lysozyme activity was assayed as described previously [36], with slight modification. Lysozyme was added to 1 ml of a suspension of *M. lysodeikticus* cells in a 0.2 M phosphate buffer (pH 6.2) at room temperature. The decrease in the absorbance at 540 nm was monitored for 1 min.

Luciferase activity was measured by using luciferin as a substrate [37]. Briefly, samples were incubated in 4 mM Mg-HEPES, Na-EDTA, 1 mg/ml BSA, 0.1 mM D-luciferin, ~20 μg/ml firefly luciferase, 20 mM K-HEPES (pH 7.8), and 50 nM ATP. The chemiluminescent product was detected by using a BioOrbit 1251 luminometer.

Bovine liver catalase activity was measured spectrophotometrically at room temperature by monitoring the changes in H_2O_2 absorbance at 240 nm as described previously [38]. The reaction was started by the addition of H_2O_2 to a final concentration of 10 mM.

Horseradish peroxidase (HRP) and choline oxidase activities were measured as described previously [39]. Samples were incubated in 250 mM NaCl, 2 mM $MgCl_2$, 5 mM Tris (pH 8.5), 0.1 mM homovanillic acid, 6 U/ml horseradish peroxidase, and 2.5 U/ml choline oxidase. Fluorescence measurements were carried out by using a Perking Elmer LS 55 fluorometer.

Succinate-cytochrome c oxido-reductase activity was measured in isolated mitochondria as described before [11].

(Na^+/K^+)ATPase activity of brain protein membranal fraction (0.1 mg/ml) was assayed following incubation for 10 min at 30ºC in a solution containing 2 mM [γ-^{32}P]ATP (10^4 cpm/mmol), 2 mM $MgCl_2$, 25 mM imidazole (pH 7.5), 10 mM KCl, 100 mM NaCl, and 0.5 mM Tris-EGTA. The [^{32}P]P_i released from [γ-^{32}P]ATP was analyzed according to Avron [40], and the radioactivity was measured in a liquid scintillation counter.

Acknowledgments

This research was supported by a research grant from B.G. Negev Technologies. We thank Dr. Noam Zilberberg for carrying out the oocyte experiment and for providing valuable suggestions.

Received: March 25, 2005
Revised: July 18, 2005
Accepted: August 10, 2005
Published: November 18, 2005

References

1. Berridge, M.J., Lipp, P., and Bootman, M.D. (2000). The versatility and universality of calcium signalling. Nat. Rev. Mol. Cell Biol. *1*, 11–21.

2. Carafoli, E. (2004). The ambivalent nature of the calcium signal. J. Endocrinol. Invest. *27*, 134–136.
3. Berridge, M.J., Bootman, M.D., and Roderick, H.L. (2003). Calcium signalling: dynamics, homeostasis and remodelling. Nat. Rev. Mol. Cell Biol. *4*, 517–529.
4. Shoshan-Barmatz, V., and Ashley, R.H. (1998). The structure, function, and cellular regulation of ryanodine-sensitive Ca^{2+} release channels. Int. Rev. Cytol. *183*, 185–270.
5. Catterall, W.A. (2000). Structure and regulation of voltage-gated Ca^{2+} channels. Annu. Rev. Cell Dev. Biol. *16*, 521–555.
6. Pozzan, T., Rizzuto, R., Volpe, P., and Meldolesi, J. (1994). Molecular and cellular physiology of intracellular calcium stores. Physiol. Rev. *74*, 595–636.
7. Blaustein, M.P., and Lederer, W.J. (1999). Sodium/calcium exchange: its physiological implications. Physiol. Rev. *79*, 763–854.
8. Brown, G.C. (1992). Control of respiration and ATP synthesis in mammalian mitochondria and cells. Biochem. J. *284*, 1–13.
9. Gunter, T.E., Buntinas, L., Sparagna, G.C., and Gunter, K.K. (1998). The Ca^{2+} transport mechanisms of mitochondria and Ca^{2+} uptake from physiological-type Ca^{2+} transients. Biochim. Biophys. Acta *1366*, 5–15.
10. Hadad, N., Zable, A.C., Abramson, J.J., and Shoshan-Barmatz, V. (1994). Ca^{2+} binding sites of the ryanodine receptor/Ca^{2+} release channel of sarcoplasmic reticulum. Low affinity binding site(s) as probed by terbium fluorescence. J. Biol. Chem. *269*, 24864–24869.
11. Gincel, D., Zaid, H., and Shoshan-Barmatz, V. (2001). Calcium binding and translocation by the voltage-dependent anion channel: a possible regulatory mechanism in mitochondrial function. Biochem. J. *358*, 147–155.
12. Ying, W.L., Emerson, J., Clarke, M.J., and Sanadi, D.R. (1991). Inhibition of mitochondrial calcium ion transport by an oxo-bridged dinuclear ruthenium ammine complex. Biochemistry *30*, 4949–4952.
13. Zazueta, C., Zafra, G., Vera, G., Sanchez, C., and Chavez, E. (1998). Advances in the purification of the mitochondrial Ca^{2+} uniporter using the labeled inhibitor ^{103}Ru360. J. Bioenerg. Biomembr. *30*, 489–498.
14. Govindaswamy, P., Ynnawar, H.P., and Kollipara, M.R. (2004). Synthesis, characterization and molecular structure of the $[(\eta^6\text{-}C_6Me_6)Ru(\mu\text{-}N_3)(N_3)]_2$ complex and its reactions with some monodentate ligands. J. Organomet. Chem. *689*, 3108–3112.
15. Vrestal, J., Kralik, F., and Soucek, J. (1960). reaktion des ruthenium(III)- und ruthenium(IV)-chlorids natriumazid. Collect. Czech. Chem. Commun. *25*, 2155–2160.
16. Brown, G.M., Callahan, R.W., and Meyer, T.J. (1975). Thermal and light-induced decomposition of azido(bis-2,2′-bipyridine) complexes of ruthenium(III). Inorg. Chem. *14*, 1915–1921.
17. Xu, L., Tripathy, A., Pasek, D.A., and Meissner, G. (1999). Ruthenium red modifies the cardiac and skeletal muscle Ca(2+) release channels (ryanodine receptors) by multiple mechanisms. J. Biol. Chem. *274*, 32680–32691.
18. Shoshan-Barmatz, V., and Gincel, D. (2003). The voltage-dependent anion channel: characterization, modulation, and role in mitochondrial function in cell life and death. Cell Biochem. Biophys. *39*, 279–292.
19. Singh, P., Salih, M., Leddy, J.J., and Tuana, B.S. (2004). The muscle-specific calmodulin-dependent protein kinase assembles with the glycolytic enzyme complex at the sarcoplasmic reticulum and modulates the activity of glyceraldehyde-3-phosphate dehydrogenase in a Ca^{2+}/calmodulin-dependent manner. J. Biol. Chem. *279*, 35176–35182.
20. Laberge, M., Szigeti, K., and Fidy, J. (2004). The charge transfer band in horseradish peroxidase correlates with heme in-plane distortions induced by calcium removal. Biopolymers *74*, 41–45.
21. Zaid, H., Abu-Hamad, S., Israelson, A., Nathan, I., and Shoshan Barmatz, V. (2005). The voltage-dependent anion channel-1 modulates apoptotic cell death. Cell Death Differ. *12*, 751–760.
22. del Arco, A., and Satrustegui, J. (2004). Identification of a novel human subfamily of mitochondrial carriers with calcium-binding domains. J. Biol. Chem. *279*, 24701–24713.
23. Czirjak, G., and Enyedi, P. (2003). Ruthenium red inhibits TASK-3 potassium channel by interconnecting glutamate 70 of the two subunits. Mol. Pharmacol. *63*, 646–652.
24. Peng, C.F., Kane, J.J., Straub, K.D., and Murphy, M.L. (1980). Improvement of mitochondrial energy production in ischemic myocardium by in vivo infusion of ruthenium red. J. Cardiovasc. Pharmacol. *2*, 45–54.
25. Tapia, R., and Velasco, I. (1997). Ruthenium red as a tool to study calcium channels, neuronal death and the function of neural pathways. Neurochem. Int. *30*, 137–147.
26. Meinicke, A.R., Bechara, E.J., and Vercesi, A.E. (1998). Ruthenium red-catalyzed degradation of peroxides can prevent mitochondrial oxidative damage induced by either tert-butyl hydroperoxide or inorganic phosphate. Arch. Biochem. Biophys. *349*, 275–280.
27. Saito, A., Seiler, S., Chu, A., and Fleischer, S. (1984). Preparation and morphology of sarcoplasmic reticulum terminal cisternae from rabbit skeletal muscle. J. Cell Biol. *99*, 875–885.
28. Lowry, O.H., Rosebrough, N.J., Farr, A.L., and Randall, R.J. (1951). Protein measurement with the Folin phenol reagent. J. Biol. Chem. *193*, 265–275.
29. Orr, I., and Shoshan-Barmatz, V. (1996). Modulation of the skeletal muscle ryanodine receptor by endogenous phosphorylation of 160/150-kDa proteins of the sarcoplasmic reticulum. Biochim. Biophys. Acta *1283*, 80–88.
30. Azoulay-Zohar, H., Israelson, A., Abu-Hamad, S., and Shoshan-Barmatz, V. (2004). In self-defence: hexokinase promotes voltage-dependent anion channel closure and prevents mitochondria-mediated apoptotic cell death. Biochem. J. *377*, 347–355.
31. Gopalakrishna, R., and Anderson, W.B. (1982). Ca^{2+}-induced hydrophobic site on calmodulin: application for purification of calmodulin by phenyl-Sepharose affinity chromatography. Biochem. Biophys. Res. Commun. *104*, 830–836.
32. Snyder, J.A., and Harrison, J.H. (1977). Frog lysozyme. V. Isolation and some physical and immunochemical properties of lysozyme isozymes of the leopard frog, Rana pipiens. J. Exp. Zool. *202*, 89–96.
33. Laemmli, U.K. (1970). Cleavage of structural proteins during the assembly of the head of bacteriophage T4. Nature *227*, 680–685.
34. Zilberberg, N., Ilan, N., and Goldstein, S.A. (2001). KCNKO: opening and closing the 2-P-domain potassium leak channel entails 'C-type' gating of the outer pore. Neuron *32*, 635–648.
35. Bowers, G.N., and McComb, R.B. (1975). Measurement of total alkaline phosphatase activity in human serum. Clin. Chem. *21*, 1988–1995.
36. Parry, R.M., Chandan, R.C., and Shahani, K.M. (1965). A rapid and sensitive assay of muramidase. Proc. Soc. Exp. Biol. Med. *119*, 384–386.
37. Holmsen, H., Holmsen, I., and Bernhardsen, A. (1966). Microdetermination of adenosine diphosphate and adenosine triphosphate in plasma with firefly luciferase system. Anal. Biochem. *17*, 456–473.
38. Durner, J., and Klessig, D.F. (1996). Salicylic acid is a modulator of tobacco and mammalian catalases. J. Biol. Chem. *271*, 28492–28501.
39. Guilbualt, G.G., Kramer, D.N., and Hackley, E. (1967). A new substrate for fluorometric determination of oxidative enzymes. Anal. Chem. *39*, 271–272.
40. Avron, M. (1960). Photophosphorylation by swiss-chard chloroplasts. Biochim. Biophys. Acta *40*, 257–272.